COMPUTATIONAL MECHANICS
WCCM VI in conjunction with APCOM'04, *Sept. 5-10, 2004, Beijing, China*

3D Finite Volume Scheme for Czochralski Crystal Growth

Jing Lu, Zi-Bing Zhang, Qi-Sheng Chen*

Institute of Mechanics, Chinese Academy of Sciences, 15 Bei-si-huan-xi Road ,Beijing, 100080, China
e-mail: qschen@imech.ac.cn

Abstract A general three-dimensional model is developed for simulation of the growth process of silicon single crystals by Czochralski technique. The numerical scheme is based on the curvilinear non-orthogonal finite volume discretization. Numerical solutions show that the flow and temperature fields in the melt are asymmetric and unsteady for 8'' silicon growth. The effects of rotation of crystal on the flow structure are studied. The rotation of crystal forms the Ekman layer in which the temperature gradient along solid/melt surface is small.

Key words: Czochralski growth, silicon single crystals, simulation

INTRODUCTION

The growth of silicon single crystals is the basis for electronic device fabrications. Czochralski (Cz) method is the most widely used technique due to its ability to meet the stringent requirements of large diameter crystals with a high degree of crystallographic perfection, low defect density and uniform dopant distribution. Currently, the Cz technology is being used to grow silicon crystals of up to 300 mm diameter.

Numerical simulation has proved to be an important and effective method for investigation of such complicated growth process especially for the growth process of 8'' and 12'' crystals. Numerical simulations of transport phenomena in Cz process have been performed by many investigators. Derby and Brown [1] developed a thermal-capillary model for heat transfer in CZ systems, which accounts for conduction-dominated heat transfer throughout the CZ system and includes calculation of the crystal/melt and melt/gas interfaces. Brown et al. [2] used finite element discretizations for the temperature field and interface shapes. Bornside et al. [3] added diffuse-gray radiation throughout the system. This approach was called the integrated thermal-capillary model (ITCM) that time. Kinney and Brown [4] used the Integrated Hydrodynamic Thermal Capillary Modeling (IHTCM) to model turbulent convection in the melt of CZ silicon systems. Lipchin and Brown [5] merged the finite-element method for solution of the ITCM and the finite-volume method for calculation of turbulent convection. Jafri et al. [6] used a finite-volume discretization to simulate laminar convection in a prototype CZ model using orthogonal staggered meshes. Zhang and Prasad [7] presented finite-volume calculations based on a discretization with a nonorthogonal curvilinear grid. They expressed the governing equations in curvilinear coordinates and transformed the computational domain to a rectangular region. Zhang et al. [8] and Prasad et al.[9] used a dynamic model to simulate CZ growth of silicon crystal. Nunes and Naraghi [10] used a radiation model called Discrete Exchange Factor (DEF) to simulate CZ growth system. The governing equations for the DEF method are obtained by discretizing the integral equations of Continuous Exchange Factor (CEF). Gevelber [11] used a lump model to model the CZ growth system. Seidl et al.[12] and Müller et al.[13] measured oxygen concentration within the melt volume using an electrochemical oxygen sensor. The oxygen sensor consists of thermocouple, solid ionic sensor and electronic melt contact. Chatterjee and Prasad [14] developed a full 3-dimensional adaptive finite volume scheme, and Chatterjee et al.[15] used it for simulation of low pressure Cz growth process. Jing and Kobayashi [16] investigated the effect of RF coil position on spoke patterns observed on the free

surface of oxide melt by 3-dimensional numerical simulations. Li et al. [17] conducted a global numerical simulations using finite element method to analyze the influence of crystal and crucible rotations on silicon melt flow and oxygen transport in a small Cz furnace.
In this paper, we used the 3D MASTRAPP [14,15] to investigate the effects of rotation of crystal and crucible on flow pattern and the temperature field in an 8'' silicon growth system.

PHYSICAL AND MATHEMATICAL MODEL

The conventional Cz method is a "batch process" in which a single crystal is grown from the melt in a crucible as shown in Fig.1. The crucible is initially filled with the polycrystalline silicon charge. Thermal energy is supplied by a heater surrounding the crucible to the silicon charge. A seed crystal is then dipped into the melt and slowly withdrawn from the melt whereby recrystallization of silicon in the form of single crystals occurs. In order to improve uniformity, the growing crystal is rotated while it is pulled from the melt, and simultaneously the crucible is rotated in the opposite direction.
In addition to buoyancy-driven natural convection which is caused by the temperature gradients in the melt, other flows such as forced convection due to the rotation of crystal, and Marangoni convection induced by non-uniform temperature distribution on the free surface are also involved in the process. The complex flow pattern becomes asymmetric for 8'' growth process, and temperature distribution is also three-dimensional.

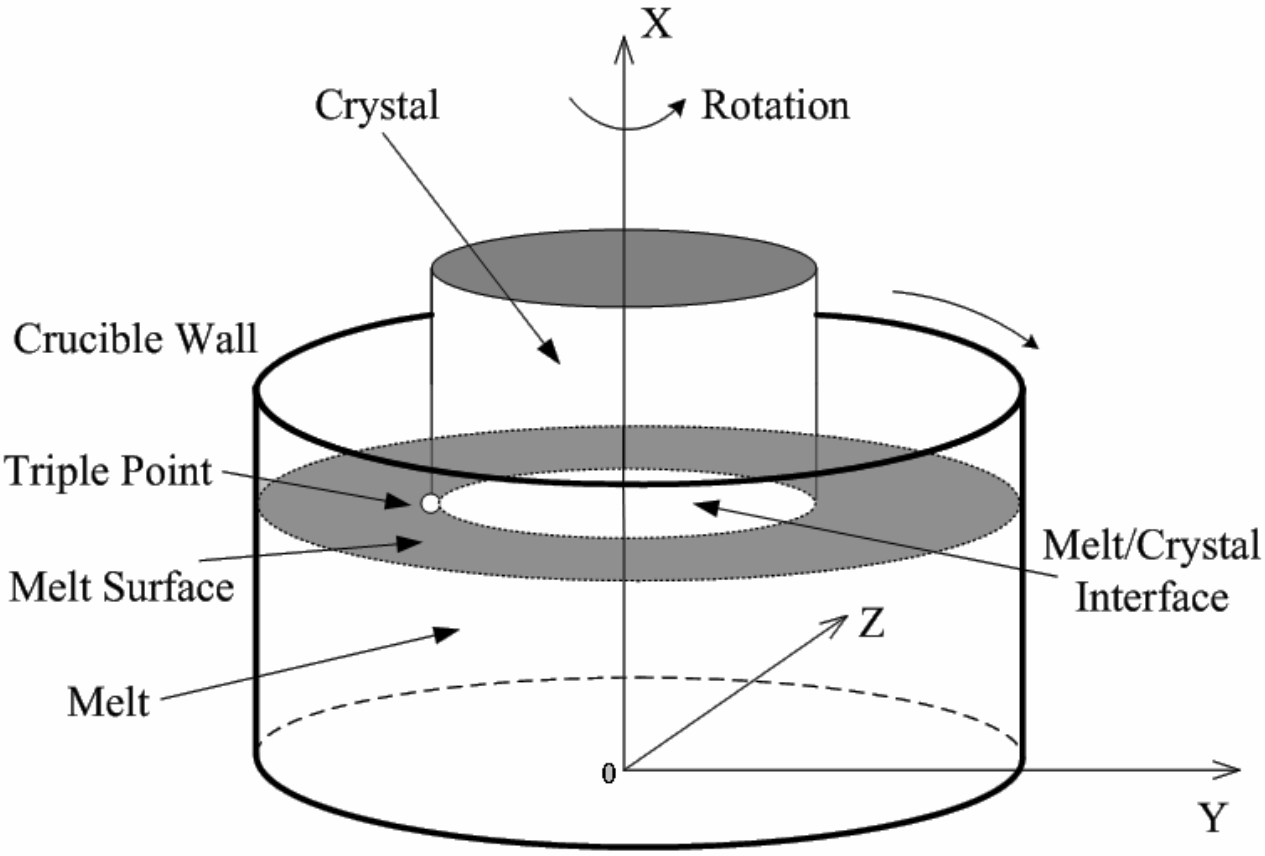

Fig. 1 Schematic of Cz growth system

1.Governing Equations A general convection-diffusion equation for any variable ϕ for an incompressible flow in a three- dimensional Cartesian coordinate system can be expressed as:

$$\frac{\partial}{\partial t}(\rho\phi)+\frac{\partial J_i}{\partial x_i}=S_\phi . \tag{1}$$

J_i is the total flux which takes the form as:

$$J_i = \rho\phi u_i - \Gamma^{\phi}\frac{\partial \phi}{\partial x_i}, \tag{2}$$

where Γ^{ϕ} is the coefficient of diffusion and S_{ϕ} is an accumulation of source terms. In the generalized non-orthogonal coordinate system, the convection-diffusion equation transforms to:

$$Ja\frac{\partial}{\partial t}(\rho\phi) + \frac{\partial}{\partial \xi_i}\left(\alpha_{\xi_i} J_{\xi_i}\right) = JaS_{\phi} + JaS_{no} + S_{aux} \qquad (i = 1,2,3) \tag{3}$$

where S_{no} is the mathematical (nonphysical) source term that arises due to the nonorthogonality of the coordinate system, S_{aux} contains the auxiliary fluxes and Ja is the Jacobian of transformation. Details about S_{aux} and Ja can be found in [14].

Similarly, the continuity equation in Cartesian system is,

$$\frac{\partial \rho}{\partial t} + \frac{\partial}{\partial x_i}(\rho u_i) = S_m . \tag{4}$$

The above equation can be written in non-orthogonal system as:

$$Ja\frac{\partial \rho}{\partial t} + \frac{\partial}{\partial \xi_i}\left(\rho\alpha_{\xi_i} u_{\xi_i}\right) = JaS_m - S_{ncont}, \tag{5}$$

where S_m is the mass source/sink term, S_{ncont} contains the auxiliary covariant fluxes analogous to S_{aux} [14].

2.Boundary Conditions The solid/liquid interface considered in this work is caused by phase change and is isothermal. For the case of solidification (also melting), Stefan condition for energy balance holds true at the interface in the following form:

$$\rho h_{sf}\tilde{V} = \left(k_s \nabla T_s - k_l \nabla T_l\right) \tag{6}$$

where $\tilde{V}$ is the interface velocity vector, h_{sf} is the latent heat, k is the thermal conductivity, T is the temperature and subscript s and l refer to solid and liquid phases, respectively.

At the free surface, the following vector equation holds tenable by assuming quasi-steady state

$$\left(p_{\infty} - p - 2\sigma H\right)\cdot \mathrm{n} + \tilde{\tilde{T}}\cdot \mathrm{n} + \frac{\partial \sigma}{\partial a}\mathrm{t} = 0 \tag{7}$$

where σ is the surface tension, $\tilde{\tilde{T}}$ the viscous stress tensor, H the mean curvature of the meniscus, a denotes the arc length, **n** the unit normal vector and **t** the unit tangent vector.

Presence of a periodic direction (ξ_3) in the cylindrical Cz system calls for specific periodic boundary condition to be imposed. In the case of a closed azimuthal direction (ξ_3), the period is 2π and the boundary condition is of the form,

$$\phi(\xi_3 = 0) = \phi(\xi_3 = 2\pi). \tag{8}$$

3.Numerical Method For the numerical solution of transport problems in domains of irregular shapes with moving phase change interfaces and boundaries, control volume method has been found to be a better option. For the numerical purpose, the discretized form of Eqs. (3) is obtained through integrating itself over the control volume as follow:

$$\frac{\rho_P (J_a)_P \phi_P - \rho_P^o (J_a^o)_P \phi_P^o}{\Delta t}\Delta\xi_1\Delta\xi_2\Delta\xi_3 + \{(\alpha_{\xi_1} J_{\xi_1})_e - (\alpha_{\xi_1} J_{\xi_1})_w\}\Delta\xi_2\Delta\xi_3 + \{(\alpha_{\xi_2} J_{\xi_2})_t$$
$$-(\alpha_{\xi_2} J_{\xi_2})_b\}\Delta\xi_1\Delta\xi_3 + \{(\alpha_{\xi_3} J_{\xi_3})_n - (\alpha_{\xi_3} J_{\xi_3})_s\}\Delta\xi_1\Delta\xi_2$$

$$= \{J_a \left(S_\phi + S_{no} \right) + S_{aux} \}_P \Delta\xi_1 \Delta\xi_2 \Delta\xi_3 \tag{9}$$

In the above equation superscript 0 denotes previous time step values, and the subscripts e, w, t, b, n, s denote the points at the center of the corresponding control volume face. The physical source term, S_ϕ, is generally linearized as:

$$\left(S_\phi \right)_P = S_C + S_P \phi_P \,. \tag{10}$$

Through applying proper operations, the final discretized form is obtained as:

$$a_P \phi_P = a_E \phi_E + a_W \phi_W + a_T \phi_T + a_B \phi_B + a_N \phi_N + a_S \phi_S + b \,, \tag{11}$$

where the details about a_P, a_E etc. can be found in [14]. Accordingly, the continuity equation, energy equation and other auxiliary equations are discretized by this means.

RESULTS AND DISCUSSION

1.Effect of Grashof number As mentioned earlier, the three main driving forces in Cz melt are buoyancy, crystal/crucible ration and surface tension on the free surface. The important non-dimensional numbers such as Prandtl number, Grashof number, Marangoni number, Crucible Reynolds number and Crystal Reynolds number are defined as:

$$\mathrm{Pr} = \nu / \alpha \,, \quad Gr = g\beta R^3 (T_w - T_f)/(\nu^2) \,, \quad Ma = \frac{\partial \sigma}{\partial T} (T_W - T_m) R / (\rho \nu \alpha) \,,$$

$$\mathrm{Re}_c = \omega_c R^2 / \nu \,, \quad \mathrm{Re}_s = \omega_s R^2 / \nu \,, \tag{12}$$

where ν is the kinetic viscosity, α the thermal diffusivity, g the gravitational acceleration, β the coefficient of thermal expansion, R the radius of crucible, T_w the temperatures at crucible wall, T_f the freezing point of Si, $\frac{\partial \sigma}{\partial T}$ the surface tension differentiation with respect to temperature, ω_c the rotation rate of crucible, and ω_s denotes the rotation rate of crystal. We will focus on the effect of Grashof number on the flow field and temperature distribution in the 8'' Cz growth system with other parameters fixed.

For 8'' Si growth, the non-dimensional parameters are $Gr = 10^9$, $\mathrm{Pr} = 0.019$, $Ma = 10^4$, $\mathrm{Re}_t = 1.8 \times 10^5$, $\mathrm{Re}_b = 60000$ for 0.48 m diameter crucible, 15 rpm rotation rate of crystal and 5 rpm rotation rate of crucible, and 150 K temperature difference between crucible temperature and freezing point.

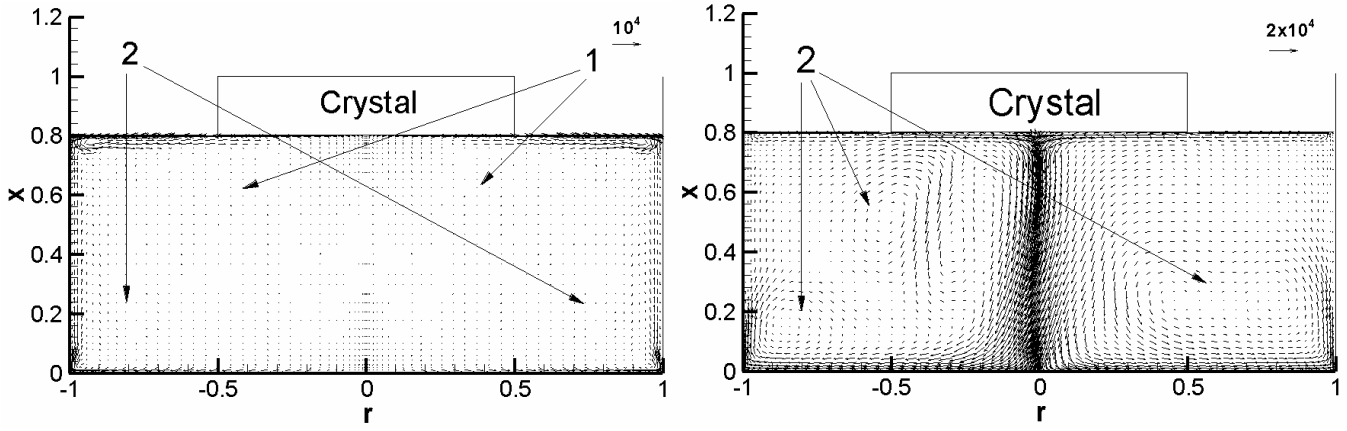

(a) (b)

Fig. 2 (a) Flow field for $Gr = 10^7$, (b) flow field for $Gr = 10^9$

The flow fields in crucible are presented in Fig. 2a and b for $Gr = 10^7$ and $Gr = 10^9$, respectively. As can be seen, there are two kinds of dominant flow patterns in the vertical plane, namely 1 and 2. Due to the crystal rotation, fluid is sucked up from underneath the crystal and pumped radially outwards. This phenomenon is known as Ekman suction which corresponds to flow pattern 1 formed near the free surface in Fig. 2. Simultaneously, the applied temperature boundary conditions result in buoyancy-driven flow in the melt, which corresponds to flow pattern near the bottom of crucible as shown in Fig. 2. A close look at the flow field reveals that for high Gr numbers ($Gr \geq 10^7$) natural convection plays an important role in the melt flow as the Ekman suction caused by crystal rotation. This tendency increases with Gr number. We can see in Fig. 2 that the zone occupied by flow pattern 2 (natural convection) is of approximately the same size as pattern 1 (Ekman suction) for $Gr = 10^7$ while it becomes much larger than pattern 1 when Gr number increases from 10^7 to 10^9.

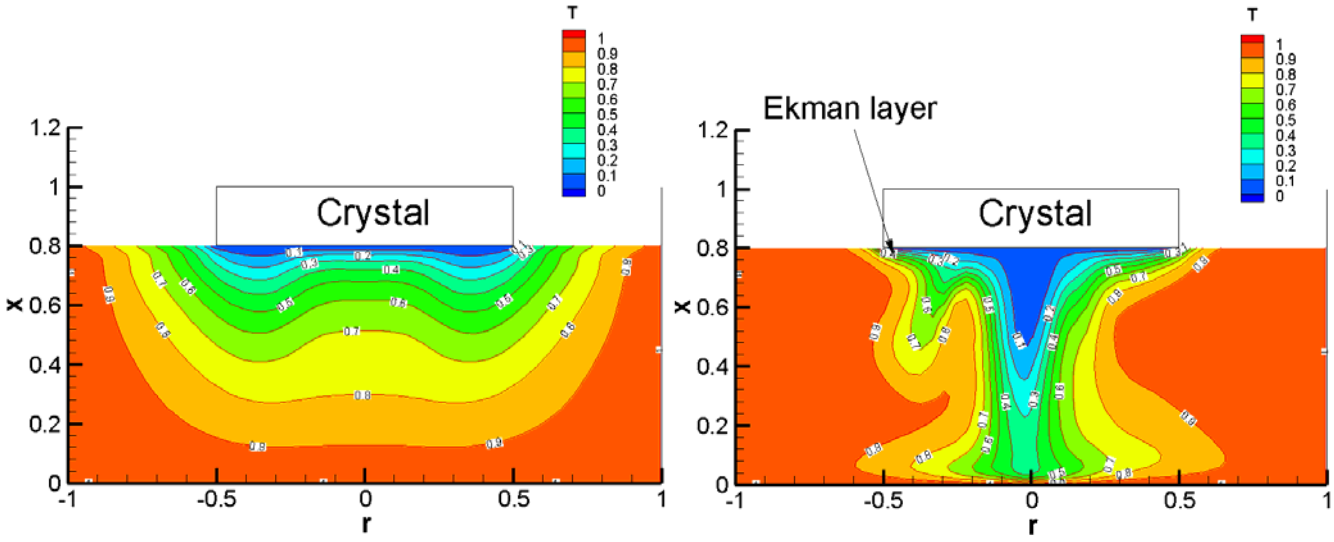

(a) (b)

Fig. 3 (a) Temperature field in the vertical plane for $Gr = 10^7$ (b) for $Gr = 10^9$

Fig. 3 (a) and (b) show the temperature distributions in the vertical plane in the melt for $Gr = 10^7$ and $Gr = 10^9$, respectively. For silicon growth, the temperature boundary conditions on the crucible side wall and bottom are maintained at $\theta = 1$ and kept constant in Cz process as demonstrated in Fig. 3. The freezing temperature, $\theta = 0$, lies at the melt/crystal interface where formation of single crystal occurs. Here we will focus on the temperature variation on the free surface to count for the Marangoni flow and the interface behavior. As can be seen from Fig. 3, there exists an outward temperature gradient along the free surface between the crucible wall and the crystal edge. The surface tension force induces an inward flow towards the crystal. By comparison between (a) and (b), it can be found that the temperature variation concentrates more at the edge of crystal for $Gr = 10^9$ than that for $Gr = 10^7$. The large temperature gradient near the triple point may have a considerable influence upon the interface behaviors from the crystal quality point of view. The rotation of crystal causes an outward flow from underneath the crystal to the triple point and the outward flow meet the inward flow just outside the triple point. The variation of temperature inside the thin Ekman layer is very small.

Axial view of velocity distribution on the melt surface for $Gr = 10^7$ and $Gr = 10^9$ are demonstrated in Fig. 4. As indicated from the flow field in Fig. 4, the velocity distribution in the core of the plane where the magnitude varies linearly with the radius is determined by the counter-clockwise rotation of the crystal, which ensures the axisymmetry of the thermal condition, while the velocity vectors at the edge of the plane correspond to the clockwise rotation of the crucible. The crystal rotation thus gives rise to centrifugal flow as is shown in Fig. 4. Effect of Gr number is then observed by keeping the rotation rate of both crystal and crucible fixed. Analyzing the velocity distributions between crystal and crucible wall, we can see that the velocity field for $Gr = 10^7$ are more uniform than that for $Gr = 10^9$. This highlights

the importance of 3-D simulation in capturing the feature of Cz process by comparison with 2-D simulations.

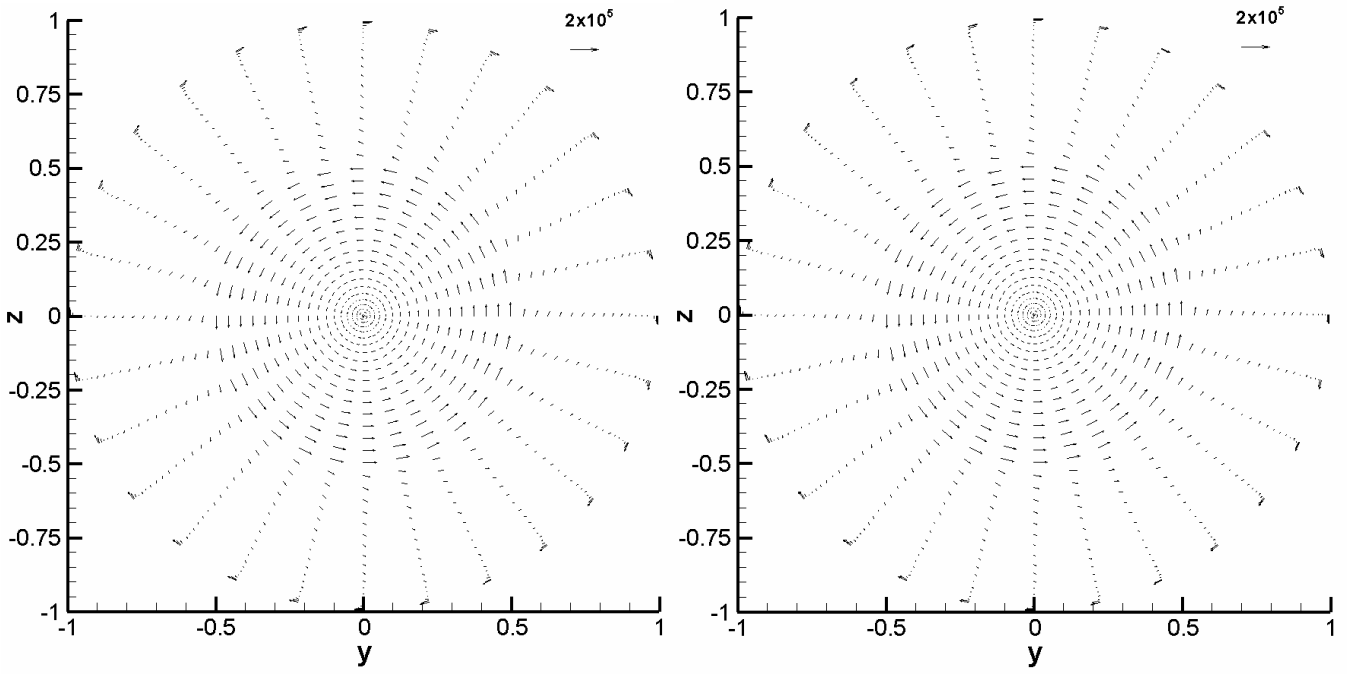

(a) (b)

Fig. 4 Velocity distribution on the melt surface (a) $Gr = 10^7$ *(b)* $Gr = 10^9$

CONCLUSIONS

The flow structure and temperature distribution in the melt are analyzed using the three-dimensional MASTRAPP, which is based on the non-orthogonal finite volume technique. The effect of Grashof number on the flow structure is studied. The Ekman layer becomes smaller when increasing the Grashof number from 10^7 to 10^9. The temperature variation inside the Ekman layer is found to be very small.

Acknowledgements The research was supported by the Knowledge Innovation Program of Chinese Academy of Sciences, and the authers would like to thank Prof. V. Prasad at the Florida International University for helpful discussions.

REFERENCES

[1] J. J. Derby, R. A. Brown, *Thermal-capillary model of Czochralski and liquid-encapsulated Czochralski crystal growth: 1. Steady-state simulation*, J. Crystal Growth 74, (1986), 605-624.

[2] R. A. Brown, P. A. Sackinger, T. A. Kinney, D. Bornside, *Integrated modeling of Czochralski crystal growth*, J. Crystal Growth 97, (1989), 99-115.

[3] D. E. Bornside, T. A. Kinney, R. A. Brown, *Finite-element/Newton method for analysis of Czochralski crystal growth with diffuse-gray radiation*, Inter. J. Meth. Engng. 30, (1990), 133-154.

[4] T. A. Kinney, R. A. Brown, *Application of turbulence modeling to integrated hydrodynamic thermal-capillary model of Czochralski crystal growth of silicon*, J. Crystal Growth 132, (1993), 551-574.

[5] A. Lipchin, R. A. Brown, *Hybrid finite-volume/finite-element simulation of heat transfer and turbulence in Czochralski crystal growth of silicon*, J. Crystal Growth 216, (2000), 192-203.

[6] I. H. Jafri, V. Prasad, A. P. Anselmo, K. P. Gupta, J. Crystal Growth 154, (1995) 280.

[7] H. Zhang, V. Prasad, J. Crystal Growth 155, (1995), 47.

[8] H. Zhang, L. L. Zheng, V. Prasad, D. J. Jr. Larson, *Diameter-controlled Czochralski growth of silicon crystals*, J. Heat Transfer, Vol. 120, (1998), 874-882.

[9] V. Prasad, H. Zhang, A. P. Anselmo, *Transport phenomena in Czochralski crystal growth process*, Advances in Heat Transfer, 30, (1997), 313-435.

[10] E. M. Nunes, M. H. N. Naraghi, *Numerical Model for Radiative Heat Transfer Analysis in Arbitrarily Shaped Axisymmetric Enclosures with Gaseous Media*, Num. Heat Transfer, Part A, Vol. 33, (1998), 495-513.

[11] M. A. Gevelber, *Dynamics and control of the Czochralski process IV. Control structure design for interface shape control and performance evaluation*, J. of Crystal Growth 139, (1994), 286-301.11.

[12] A. Seidl, R. Marten, G. Muller, *Oxygen distribution in Czochralski silicon melts measured by an electrochemical oxygen sensor*, materials Science and Engineering B36, (1996), 46-49.

[13] G. Müller, A. Mühe, R. Backofen, E. Tomzig, W. V. Ammon, *Study of Oxygen transport in Cz growth of silicon*, Microelectronics Engineering 1, (1999), 135-147.

[14] A. Chatterjee, V. Prasad, *A full 3-dimensional adaptive finite volume scheme for transport and phase-change processes, Part 1: Formulation and validation*, Num. Heat Transfer, Part A, 37, (2000), 801-822.

[15] A. Chatterjee, V. Prasad, D. Sun, *A full 3-dimensional adaptive finite volume scheme for transport and phase-change processes, Part II: Application to crystal growth*, Num. Heat Transfer, Part A, 37, (2000), 823-843.

[16] C. J. Jing, M. Kobayashi, *Effect of RF coil position on spoke pattern on oxide melt surface in Czochralski crystal growth*, J. of Crystal Growth 252, (2003), 550-559.

[17] You-Rong Li, Nobuyuki Imaishi, Yasunobu Akiyama, *Global analysis of a small Czochralski furnace with rotating crystal and crucible*, J. of Crystal Growth 255, (2003), 81-92.